Synergistic tumor suppression by combined inhibition of telomerase and CDKN1A

Romi Gupta[a], Yuying Dong[a], Peter D. Solomon[a], Hiromi I. Wettersten[b], Christopher J. Cheng[c,d], Jin-Na Min[a,e], Jeremy Henson[f,g], Shaillay Kumar Dogra[h], Sung H. Hwang[i], Bruce D. Hammock[i], Lihua J. Zhu[j], Roger R. Reddel[f,g], W. Mark Saltzman[c], Robert H. Weiss[b,k], Sandy Chang[a,e], Michael R. Green[l,1], and Narendra Wajapeyee[a,1]

Departments of [a]Pathology and [e]Laboratory Medicine, Yale University School of Medicine, New Haven, CT 06510; [i]Department of Entomology and [b]Division of Nephrology, Department of Internal Medicine, University of California, Davis, California 95616; Departments of [c]Biomedical Engineering and [d]Molecular Biophysics and Biochemistry, Yale University, New Haven, CT 06511; [f]Sydney Medical School, University of Sydney, NSW 2006, Australia; [g]Cancer Research Unit, Children's Medical Research Institute, Westmead, NSW 2145, Australia; [h]Singapore Institute of Clinical Sciences, Agency for Science Technology and Research (A*STAR), Brenner Center for Molecular Medicine, Singapore 117609; [i]Howard Hughes Medical Institute and [j]Programs in Gene Function and Expression and Molecular Medicine, University of Massachusetts Medical School, Massachusetts 01605; and [k]Department of Medicine, Mather VA Medical Center, Sacramento, CA 9565

Tumor suppressor p53 plays an important role in mediating growth inhibition upon telomere dysfunction. Here, we show that loss of the p53 target gene cyclin-dependent kinase inhibitor 1A (*CDKN1A*, also known as *p21*^WAF1/CIP1^) increases apoptosis induction following telomerase inhibition in a variety of cancer cell lines and mouse xenografts. This effect is highly specific to p21, as loss of other checkpoint proteins and CDK inhibitors did not affect apoptosis. In telomerase, inhibited cell loss of p21 leads to E2F1- and p53-mediated transcriptional activation of p53-upregulated modulator of apoptosis, resulting in increased apoptosis. Combined genetic or pharmacological inhibition of telomerase and p21 synergistically suppresses tumor growth. Furthermore, we demonstrate that simultaneous inhibition of telomerase and p21 also suppresses growth of tumors containing mutant p53 following pharmacological restoration of p53 activity. Collectively, our results establish that inactivation of p21 leads to increased apoptosis upon telomerase inhibition and thus identify a genetic vulnerability that can be exploited to treat many human cancers containing either wild-type or mutant p53.

A prominent feature that distinguishes cancer cells from their normal counterparts is the expression of telomerase. Telomerase is a specialized ribonucleoprotein reverse transcriptase that synthesizes the telomeric DNA ends to maintain telomere length (1). During early tumorigenesis, telomerase expression is necessary to bypass replicative senescence, enabling immortalization of human cells (2). Notably, telomerase also represents an attractive target for cancer therapy because a large majority of cancer cells depend on telomerase expression for survival. Accordingly, genetic or pharmacological inhibition of telomerase has been shown to suppress growth of cancer cells (3). In fact, the telomerase inhibitor imetelstat, an oligonucleotide that inhibits telomerase activity by binding to the RNA component of human telomerase RNA (hTR), has advanced to the clinic for treatment of various hematological malignancies and solid tumors. To date, however, telomerase-based monotherapies have not been successful, underscoring the need to understand in greater detail how cancer cells respond to telomerase inhibition.

Previous studies have shown that the tumor suppressor p53 pathway plays a central role in regulating the cellular response to telomerase inhibition and telomere shortening (4). Genetic deletion of p53 in mice or RNA interference (RNAi)-mediated inhibition of p53 counteracts the growth suppression that occurs following telomerase inhibition. Furthermore, p53 loss cooperates with telomerase dysfunction to promote tumorigenesis (4). CDKN1A (also known as p21^WAF1/CIP1^) is a cyclin-dependent kinase inhibitor and a direct transcriptional target of p53 (5, 6). p21 mediates several important physiological effects of p53, including DNA-damage–induced cell cycle checkpoints (7, 8). In ad-

dition to its role in cell cycle regulation, p21 has been shown in a variety of studies to repress apoptosis (9–13).

Here, we study the role of p21 in the context of telomerase inhibition. We find that abrogation of p21 function induces apoptosis in cancer cells following telomerase inhibition through up-regulation of p53-upregulated modulator of apoptosis (PUMA), a proapoptotic protein. Based upon these results, we go on to show that simultaneous genetic or pharmacological inhibition of telomerase and p21 can synergistically suppress tumor growth, even in p53 pathway-defective cancers.

Results

Induction of Apoptosis Following Telomerase Inhibition in Cancer Cells Lacking p21. As described above, p53 is known to play an important role in the cellular response to telomere dysfunction, and *p21* is a major target of p53. However, the specific role of p21 in human cancer cells with dysfunctional telomeres has not been examined. Therefore, we asked whether cancer cells respond differently to telomerase inhibition and consequential telomere shortening in the presence or absence of p21. Toward this end, we treated HCT116 cells and HCT116 *p21* knockout cells (HCT116 p21KO) with the telomerase inhibitor imetelstat (14). We found that imetelstat inhibited proliferation of HCT116 p21KO cells
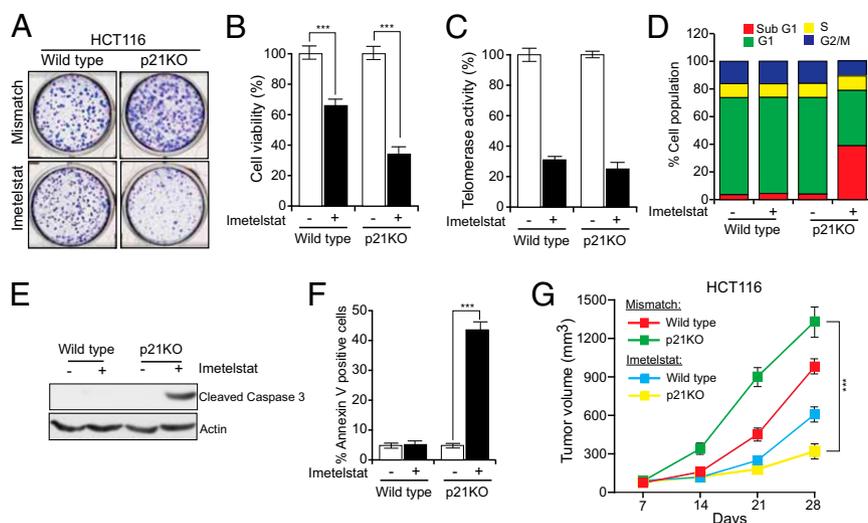
Fig. 1. Telomerase inhibition induces apoptosis in the absence of *p21*. Indicated cell lines were treated with mismatch oligonucleotide or imetelstat for 6 wk. (*A*) Crystal violet staining of HCT116 wild-type and p21KO colonies. Representative wells are shown. (*B*) Relative cell viability was monitored by trypan blue exclusion assay. (*C*) Telomerase activities of HCT116 wild-type and HCT116 p21KO cells. (*D*) Flow cytometry analysis to monitor apoptotic cells. (*E*) Cleaved caspase 3 immunoblot to measure apoptosis. Actin was used as a loading control. (*F*) % Annexin V–FITC–positive cells under indicated treatment conditions. (*G*) Average tumor volumes for indicated cell lines are presented at indicated conditions. ***$P < 0.0001$.

much more strongly than that of HCT116 cells (Fig. 1 *A* and *B*). Notably, telomerase inhibition in HCT116 and HCT116 p21KO cells was comparable (Fig. 1*C*). Additional experiments revealed that growth inhibition of HCT116 p21KO cells was largely due to increased apoptosis (Fig. 1 *D–F*). Furthermore, we knocked down telomerase using two different short hairpin RNAs (shRNAs) in HCT116 and HCT116 p21KO cells. Similar to the results with imetelstat, we found that shRNA-mediated knockdown of telomerase inhibited proliferation of HCT116 p21KO cells more efficiently than that of HCT116 cells (*SI Appendix*, Fig. S1).

Guided by these cell culture results, we injected HCT116 or HCT116 p21KO cells s.c. into athymic nude mice and monitored tumor growth after treatment with imetelstat or a control mismatch oligonucleotide. Similar to the cell culture results, we found that imetelstat inhibited growth of HCT116 p21KO tumors more effectively than that of HCT116 tumors (4.0-fold inhibition for HCT116 p21KO versus 1.6-fold inhibition for HCT116 cells) (Fig. 1*G*).

To determine the generality of these results, we used RNAi to knock down *p21* in HCT116 cells and the unrelated ACHN (renal) and RKO (colorectal) human cancer cell lines (*SI Appendix*, Figs. S2 and S3). Cells transduced with *p21* shRNAs or a nonspecific control shRNA were treated with imetelstat or a mismatch oligonucleotide and monitored for proliferation. As observed in HCT116 p21KO cells, shRNA-mediated knockdown of *p21* enhanced growth inhibition by imetelstat in HCT116, ACHN, and RKO cells by inducing apoptosis (*SI Appendix*, Fig. S2 and Fig. 2 *A–J*). In complete agreement with our cell culture experiments, we observed that treatment with imetelstat inhibited the growth of *p21* shRNA expressing ACHN and RKO tumors in mice much more strongly than ACHN and RKO tumors expressing a nonspecific control shRNA (Fig. 2 *K* and *L*).

We also analyzed the imetelstat sensitivity of four additional human cancer cell lines—LOX IMVI (melanoma), UACC62 (melanoma), CAKI (clear cell carcinoma), and NCI H460 (lung adenocarcinoma)—that express either high or low levels of p21. Similar to the results presented above, cell lines expressing a low level of p21 (NCI H460) were sensitive to imetelstat-mediated growth inhibition, whereas cell lines expressing a high level of p21 (LOX IMVI, UACC62, and CAKI) were not (*SI Appendix*, Fig. S3). In fact, proliferation of imetelstat-treated LOX IMVI

and UACC62 cells was higher than that of the mismatch oligonucleotide-treated cells (*SI Appendix*, Fig. S3), possibly due to the activation of Alternative Lengthening of Telomeres (ALT) pathway (*SI Appendix*, Fig. S3). Taken together, these results indicate that loss of p21 sensitizes diverse cancer cell lines to tumor inhibition and apoptosis following abrogation of telomerase activity.

Role of Other Checkpoint Proteins and Other CDK Inhibitors in Telomerase Inhibition-Induced Apoptosis. p53 is necessary for DNA-damage–mediated transcriptional activation of *p21* (15), and genetic deletion of p21 abrogates p53-mediated G1 and G2/M checkpoints (8, 16). We therefore asked whether knockdown of other checkpoint proteins also sensitizes cancer cells to telomerase inhibition-mediated apoptosis. Toward this end, we analyzed two previously described checkpoint proteins, mediator of DNA damage checkpoint protein 1 (MDC1) and Nijmegen breakage syndrome 1 (NBS1) (17–19). Notably, MDC1 has been shown to have a role in detection and repair of human and mouse telomeres that are rendered dysfunctional through inhibition of TRF2 (20), whereas MRE11–RAD50–NBS1 has been shown to associate with TRF2 and human telomeres (21).

To test the effect of these proteins, *MDC1* and *NBS1* were knocked down in HCT116 cells, followed by treatment with imetelstat. As a control, HCT116 cells expressing a nonspecific shRNA were analyzed in parallel. In contrast to the results with *p21*, depletion of NBS1 or MDC1 did not increase the sensitivity of HCT116 cells to imetelstat-mediated growth suppression (*SI Appendix*, Fig. S4).

Additionally, we also tested the role of a second cyclin-dependent kinase inhibitor CDKN1B (also known as p27). In contrast to p21 loss, knockdown of *p27* did not sensitize HCT116 cells to imetelstat-induced apoptosis (*SI Appendix*, Fig. S5). Furthermore, although the cancer cell lines used in our studies lacked *CDKN2A* (also known as p16) (*SI Appendix*, Table S1) (22, 23), they varied in their response to imetelstat. These results indicate that p16 expression also does not determine the response of cancer cells to telomerase inhibition. Collectively, these results show that unlike p21, loss of other checkpoint proteins (e.g., MDC1 and NBS1) or other CDK inhibitors (e.g., p27 and p16) does not cooperate with imetelstat to induce apoptosis.
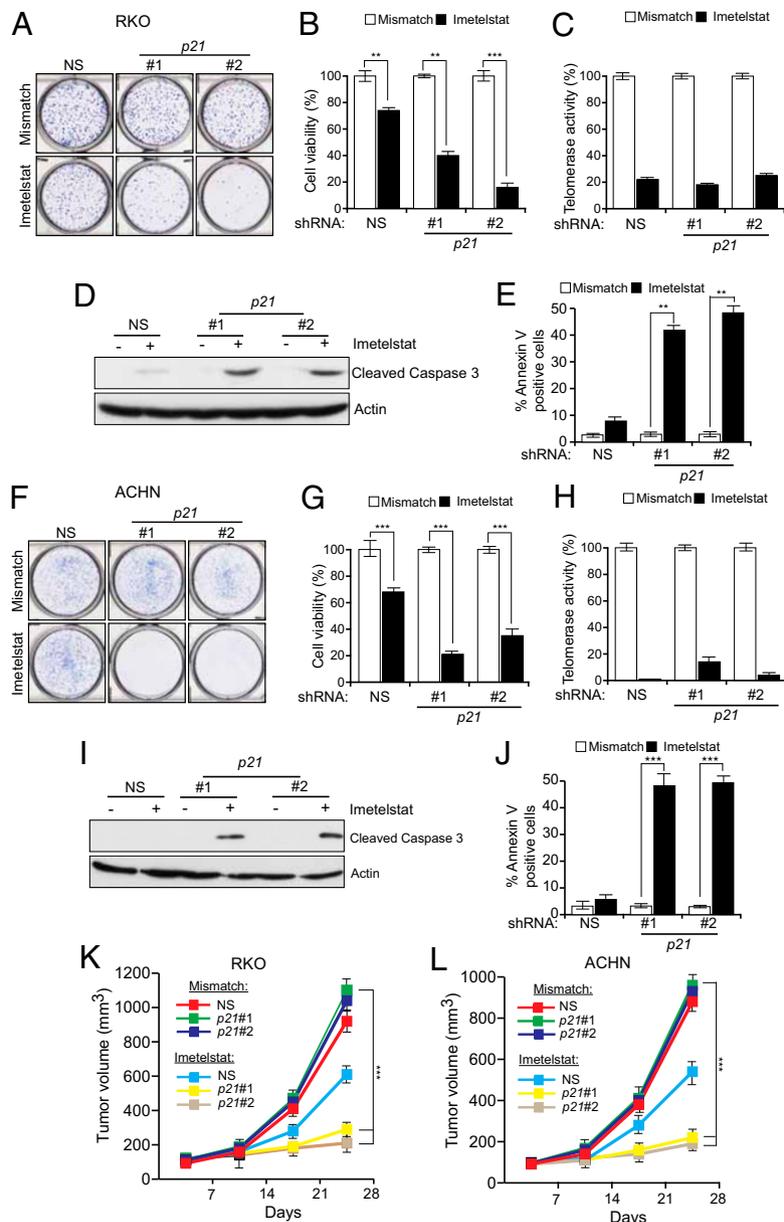
Fig. 2. shRNA-mediated *p21* knockdown in unrelated human cancer cell lines sensitizes them to telomerase inhibition-mediated apoptosis. Analysis of RKO (*A–E*) and ACHN (*F–J*) cells stably transduced with nonspecific control (NS) or two different *p21* shRNAs. (*A–E* and *F–J*) Cells were treated with mismatch oligonucleotide or with imetelstat for 6 wk. (*A* and *F*) Colony formation monitored by crystal violet staining. (*B* and *G*) Cell viability was measured by trypan blue exclusion assay. Cell viability relative to mismatch oligonucleotide is plotted. (*C* and *H*) Telomerase activity as measured by the TRAP assay and plotted relative to the mismatch oligonucleotide. (*D* and *I*) Cleaved caspase 3 immunoblot to measure apoptosis. Actin was used as a loading control. (*E* and *J*) % Annexin V–FITC–positive cells under indicated treatment conditions. (*K* and *L*) Average tumor volumes for indicated cell lines for indicated conditions are shown. **$P < 0.001$; ***$P < 0.0001$.

We also tested whether a general cellular stress could cooperate with either imetelstat treatment or p21 loss to induce apoptosis. Our results show that tunicamycin, which induces ER stress, had no cooperative effect with either imetelstat treatment or p21 loss on cell proliferation or apoptosis (*SI Appendix,* Fig. S6).

Apoptosis Induction After Telomerase Inhibition in Cancer Cells Lacking p21 Does Not Involve Telomere Attrition or ALT. We next sought to understand the mechanism by which apoptosis is induced by imetelstat in HCT116 p21KO cells. First, we examined whether loss of p21 affects the ability of imetelstat to induce telomere shortening. *SI Appendix,* Fig. S7 *A–D* shows that there was no significant difference between imetelstat-treated HCT116

and HCT116 p21KO cells in either the extent of telomere shortening or the number of signal-free chromosomal ends. Although in most cancer cells maintenance of telomere length depends on telomerase activity, in about 10–15% of cancers telomere length is maintained through an alternative ALT pathway (24). The mechanism of ALT has not been fully elucidated, however a general consensus is that it requires homologous recombination (24). Furthermore, previous studies have shown that, following telomerase inhibition, cancer cells can survive by activating the ALT pathway (24, 25). We therefore tested whether the ALT pathway was more active in HCT116 cells than HCT116 p21KO cells after imetelstat treatment by monitoring partially single-stranded telomeric (CCCTAA)$_n$ DNA circles (C-circles), a characteristic, quan-

tifiable marker of ALT activity (26). As expected, the previously described ALT-positive osteosarcoma cell line U2OS produced C-circles, whereas ALT-negative HeLa cells did not (*SI Appendix*, Fig. S7E). Notably, we did not detect C-circles in either HCT116 or HCT116 p21KO cells, before or after imetelstat treatment, indicating that ALT activity does not explain the differential response to imetelstat. As an additional control, we analyzed the effect of telomerase inhibition in cancer cell line U2OS, in which the ALT pathway is active, and thus these cells do not depend upon telomerase expression for survival (27). As expected, treatment with imetelstat did not affect the proliferation of U2OS cells in the absence or presence of *p21* shRNAs (*SI Appendix*, Fig. S8). Collectively, these results further confirm that imetelstat inhibits telomerase activity to prevent growth of cancer cells that are dependent upon telomerase activity for survival.

P53- and E2F1-Mediated PUMA Activation in Cells Lacking p21 After Telomerase Inhibition. In addition to promoting cell cycle arrest in response to DNA damage, the tumor suppressor p53 activates proapoptotic genes such as *BAX*, *BAK*, and *PUMA* to induce apoptosis (28–32). We therefore monitored expression of *BAX*, *BAK*, and *PUMA* in HCT116 and HCT116 p21KO cells treated with imetelstat. Unexpectedly, imetelstat treatment induced *PUMA* expression to substantially higher levels in HCT116 p21KO cells compared with HCT116 cells (Fig. 3 *A* and *B*). Likewise, shRNA-mediated knockdown of *p21* in RKO and ACHN cells led to a large increase in PUMA expression following imetelstat treatment (*SI*

Appendix, Fig. S9 *A* and *B* as well as *G* and *H*). By contrast, following imetelstat treatment, *BAK* expression was actually higher in HCT116 cells than in HCT116 p21KO cells, and *BAX* expression was comparable in the two cell lines (Fig. 3 *A* and *B*).

Previous studies have shown that the E2F1 transcription factor is an activator of *PUMA* transcription and that p21 can negatively regulate E2F1 activity (33, 34). These two findings suggested that E2F1 might activate *PUMA* expression in HCT116 p21KO cells following imetelstat treatment. Consistent with this idea, following knockdown of *E2F1* in HCT116 p21KO cells, imetelstat treatment no longer activated *PUMA* expression (Fig. 3 *C* and *D*). Furthermore, following shRNA-mediated knockdown of *E2F1* in HCT116 p21KO cells, imetelstat failed to inhibit cellular proliferation (Fig. 3*E* and *SI Appendix*, Fig. S10) or efficiently induce apoptosis (Fig. 3 *F* and *G*). Likewise, *PUMA* transcription was not activated by imetelstat in HCT116 p53KO cells following *p21* knockdown (Fig. 3 *H* and *I*). *PUMA* expression was comparable in imetelstat-treated cells containing or depleted of the checkpoint proteins *NBS1* and *MDC1* (*SI Appendix*, Fig. S4 *F* and *L*) as well as in cells depleted of the CDK inhibitor p27 (*SI Appendix*, Fig. S5F), again confirming the specific role of p21 in regulating apoptosis following telomerase inhibition. Thus, in the absence of p21, E2F1 and p53 activate *PUMA* expression in telomerase-inhibited cells.

Previous work has shown that p53 deficiency prevents the growth inhibitory effects of telomere dysfunction (35). Indeed, we found that HCT116 p53KO cells were more resistant to
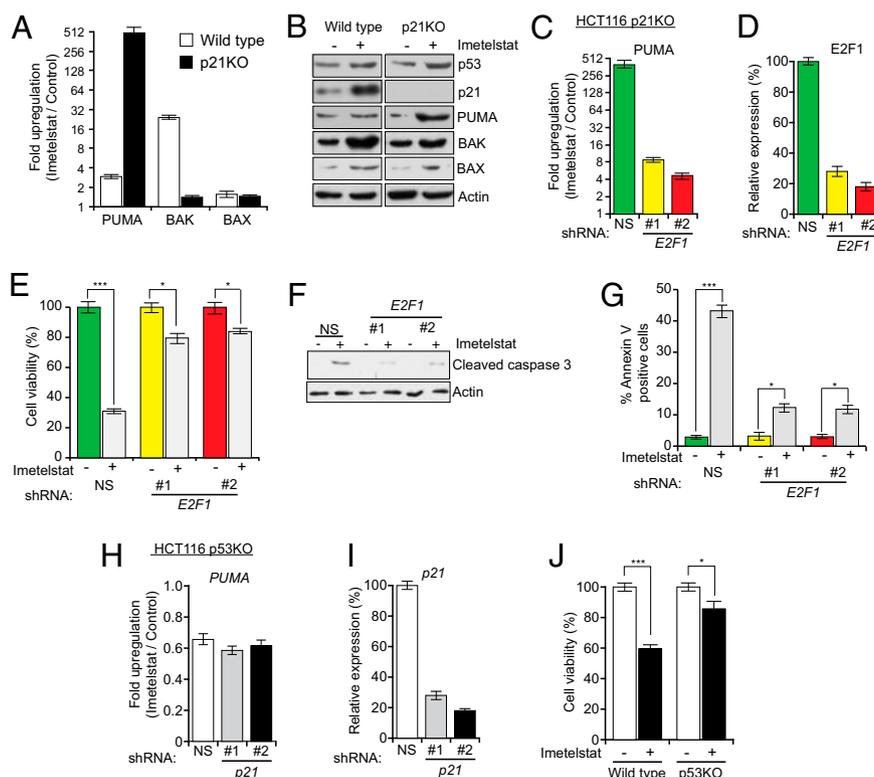

Fig. 3. Telomerase inhibition activates E2F1- and p53-dependent *PUMA* transcription in the absence of *p21*. Indicated cell lines were treated with either a mismatch oligonucleotide or imetelstat. (*A*) Fold change in *PUMA*, *BAK*, and *BAX* transcript levels measured by quantitative RT-PCR (qRT-PCR) after 6 wk of treatment. (*B*) Immunoblot analysis was performed for indicated proteins. (*C*) *PUMA* expression was measured in imetelstat-treated HCT116 p21KO cells after *E2F1* or control (NS) shRNA knockdown. (*D*) *E2F1* knockdown was confirmed by qRT-PCR. (*E*) Relative cell viability was measured by trypan blue exclusion assay. (*F*) Cleaved caspase 3 was measured by immunoblot in mismatch oligonucleotide or imetelstat-treated HCT116 p21KO cells after *E2F1* or control (NS) shRNA knockdown. Actin expression was monitored as a control. (*G*) Annexin V–FITC–positive cells were quantified by FACS analysis in mismatch oligonucleotide or imetelstat-treated HCT116 p21KO cells after *E2F1* or control (NS) shRNA knockdown. (*H*) *PUMA* expression in imetelstat-treated HCT116 p53KO after *p21* or control (NS) shRNA knockdown. (*I*) *p21* knockdown was confirmed by qRT-PCR. (*J*) Cell viability of HCT116 wild-type and p53KO cells after 6 wk of imetelstat treatment monitored by trypan blue exclusion. *P < 0.01; ***P < 0.0001.

GENETICS

imetelstat than parental HCT116 cells (Fig. 3*J* and *SI Appendix*, Fig. S10). These results led us to hypothesize that p53- and E2F1-dependent activation of *PUMA* transcription is necessary for apoptosis induction following telomerase inhibition in p21KO cells. To test this idea, we used an HCT116 cell line bearing homozygous deletions in both *p21* and *PUMA* (HCT116 *p21/PUMA* DKO). Notably, loss of *PUMA* prevented growth inhibition and apoptosis following treatment of HCT116 p21KO cells with imetelstat (Fig. 4 *A–C*). Likewise, simultaneous shRNA-mediated knockdown of *PUMA* (*SI Appendix*, Fig. S9 *C and I*) counteracted imetelstat-mediated growth inhibition in RKO and ACHN cells expressing a *p21* shRNA (*SI Appendix*, Fig. S9 *D–F and J–L*).

To test whether loss of *PUMA* also rescued imetelstat-mediated growth inhibition in vivo, we injected HCT116, HCT116 p21KO, and HCT116 p21/PUMA DKO cells into the flanks of nude mice followed by treatment with either imetelstat or a mismatch oligonucleotide. Consistent with the cell culture results, imetelstat did not suppress growth of tumors lacking both *p21* and *PUMA* (Fig. 4*D*). Analysis of tumors by terminal deoxynucleotidyl

transferase-mediated dUTP nick end labeling (TUNEL) showed that after imetelstat treatment, apoptosis was significantly higher in p21KO tumors compared with HCT116 p21/PUMA DKO tumors (Fig. 4 *E* and *F*). Collectively, these results demonstrate that in the absence of *p21*, telomerase inhibition leads to E2F1- and p53-dependent transcriptional activation of *PUMA*, resulting in apoptosis.

To establish the generality of the *PUMA* transcriptional activation mechanism, we analyzed five human cancer cell lines with differing levels of p21 expression. We found that in a cell line with low p21 levels (NCI H460) transcriptional activation of *PUMA* after imetelstat treatment was substantially higher than that of cell lines with high p21 levels (LOX IMVI, UACC62, and CAKI; *SI Appendix*, Fig. S11*A*). Furthermore, knockdown of *PUMA* (*SI Appendix*, Fig. S11*B*) rescued NCI H460 cells from imetelstat-mediated growth inhibition (*SI Appendix*, Fig. S11 *C and D*). Collectively, these results show that activation of *PUMA* is necessary for apoptosis induction in cells lacking p21 after telomerase inhibition.
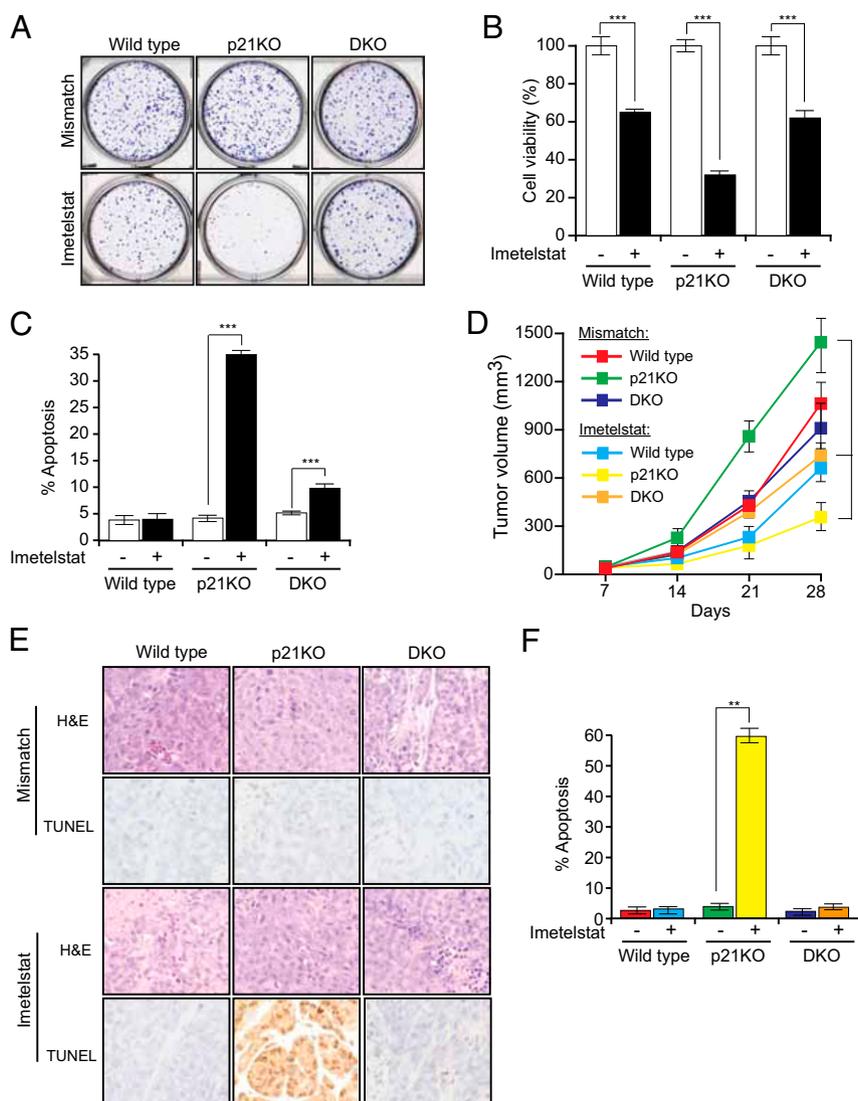

Fig. 4. PUMA induces apoptosis when telomerase is inhibited in the absence of *p21*. Indicated cell lines were treated with either a mismatch oligonucleotide or imetelstat for 6 wk. (*A*) Crystal violet staining of HCT116 wild-type, p21KO, and p21/PUMA DKO colonies. Representative wells are shown. (*B*) Relative cell viability of the indicated cells measured by trypan blue exclusion assay. (*C*) Apoptosis was measured by FACS analysis. (*D*) Average tumor volumes from mice treated with either mismatch oligonucleotide or imetelstat for indicated conditions for noted cell lines are shown. (*E*) TUNEL assay measuring apoptosis for indicated tumor samples was performed. (*F*) Quantitation of TUNEL-positive cells is shown. **$P < 0.001$; ***$P < 0.0001$.

Synergistic Tumor Suppression by RNAi-Mediated p21 Depletion and Imetelstat Treatment. The results described above suggested that simultaneous inhibition of p21 and telomerase could synergistically suppress tumor growth. We therefore carried out a series of experiments in which p21 function was abrogated using different approaches and telomerase was inhibited with imetelstat. In the first approach, we used a polymer nanoparticle-based system to deliver a *p21* small interfering RNA (siRNA) (36, 37). These poly(lactic-*co*-glycolic acid) (PLGA) nanoparticles were coated with the PEGylated cell-penetrating peptide, N terminus of the CPP penetratin (ANTP), and loaded with a p21 siRNA. As a control, a nonspecific negative control siRNA was similarly encapsulated into modified PLGA nanoparticles. We then s.c. injected HCT116 and ACHN cells into athymic nude mice and systemically treated the mice with imetelstat and nanoparticles encapsulated in siRNA. In good agreement with our cell culture results, the combination of a p21 siRNA and imetelstat resulted in significantly stronger tumor suppression compared with imetelstat alone (*SI Appendix*, Fig. S12 *A* and *B* and Table S2). Furthermore, as expected, analyses of tumor lysates revealed reduced p21 expression in *p21* siRNA nanoparticle-injected tumors (*SI Appendix*, Fig. S12 *C* and *D*), increased apoptosis upon simultaneous inhibition of p21 and telomerase (*SI Appendix*, Fig. S12 *C* and *D*), and reduced telomerase activity in imetelstat-treated tumor samples (*SI Appendix*, Fig. S12 *E* and *F*).

Synergistic Tumor Suppression by Pharmacological Inhibition of Telomerase and p21. The *p21* siRNA results described above provide proof-of-principle that systemic in vivo targeting of p21 can substantially enhance tumor suppression when combined with telomerase inhibition. We next performed experiments in which p21 function was abrogated by pharmacological inhibition in conjunction with imetelstat treatment. We first inhibited p21 expression in HCT116 cells using sorafenib (Fig. 5*A*), which promotes proteasome-mediated degradation of p21 (38). As predicted, we found that sorafenib sensitized cells to imetelstat-mediated growth inhibition and apoptosis induction (Fig. 5 *B–D*). Notably, reintroduction of *p21* in HCT116 cells treated with imetelstat and sorafenib substantially counteracted growth inhibition and apoptosis induction (Fig. 5 *E–H*), confirming that sorafenib functions by down-regulating p21 activity. Next, we tested the combined effect of imetelstat and sorafenib in suppressing tumor growth in mouse xenografts. We found that simultaneous treatment with imetelstat and sorafenib was substantially more effective at suppressing growth of HCT116 xenografts than either drug alone and thus functions in a synergistic manner (Fig. 5*I* and *SI Appendix*, Table S2).

Toxicity analyses revealed that there were no significant differences in the body weight or alanine aminotransferase (ALT), aspartate aminotransferase (AST), alkaline phosphatase (AP), whole blood counts, and renal activity markers in mice that were treated with imetelstat sorafenib, or both, in comparison with the control group (*SI Appendix*, Fig. S13). Finally, to determine the generality of these results, we analyzed the effect of combined imetelstat and sorafenib treatment on xenografts formed from five additional human cancer cell lines representing four different tissue origins. Notably, in all cases, treatment with both imetelstat and sorafenib was substantially more effective at suppressing tumor growth than either drug alone (*SI Appendix*, Fig. S14 and Table S2).
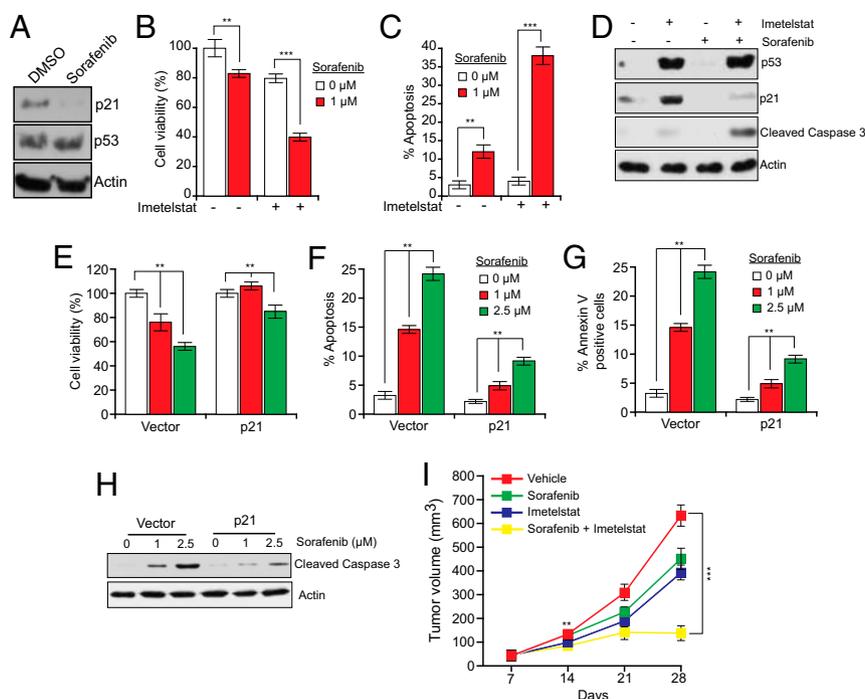

Fig. 5. Simultaneous pharmacological inhibition of p21 by sorafenib and telomerase prevents tumor growth in mice. (*A*) Immunoblot of p21 expression in HCT116 cells treated with DMSO or sorafenib (1 μM) for 24 h. (*B*) Relative cell viability measured by trypan blue exclusion assay of HCT116 cells treated with imetelstat and sorafenib. (*C*) Apoptosis of HCT116 cells treated with imetelstat and sorafenib was measured by FACS analysis. (*D*) Immunoblot for indicated proteins in HCT116 cells treated with sorafenib, imetelstat, or both. (*E*) Relative cell viability measured by trypan blue exclusion assay of imetelstat-treated HCT116 cells transfected with control or *p21* expression vectors and then treated with sorafenib. (*F*) Apoptosis measured by FACS analysis of imetelstat-treated HCT116 cells transfected with control or *p21* expression vectors and then treated with sorafenib. (*G*) Annexin V–FITC–positive cells were quantified by FACS analysis of imetelstat-treated HCT116 cells transfected with control or *p21* expression vectors and then treated with sorafenib. (*H*) Cleaved caspase 3 was measured by immunoblot in imetelstat-treated HCT116 cells transfected with control or *p21* expression vectors and then treated with sorafenib. (*I*) Average tumor volumes from mice treated with vehicle, sorafenib alone, imetelstat alone, or both drugs. **$P < 0.001$; ***$P < 0.0001$.

Sorafenib has been shown to have cellular targets other than p21, including BRAF and VEGF (39). Therefore, we asked whether an alternative pharmacological inhibitor that more selectively targets p21 expression can, like sorafenib, cooperate with imetelstat to suppress tumor growth. Toward this end, we used a recently identified pharmacological p21 inhibitor, UC2288 (Fig. 6A), which down-regulates p21 levels through transcriptional and post-transcriptional mechanisms (40). Furthermore, unlike Sorafenib, UC2288 does not inhibit RAF kinase or VEGF activities (40). In agreement with previous studies, we observed that treatment of cancer cells with UC2288 led to decreased p21 levels (Fig. 6B). Furthermore, whereas UC2288 alone had only modest growth inhibitory effects, combining UC2288 with imetelstat potently inhibited cancer cell growth by inducing apoptosis (Fig. 6 C–E). The ability of UC2288 to inhibit growth was largely dependent upon its ability to down-regulate p21 expression, because ectopic expression of p21 counteracted growth inhibition and apoptosis induction in UC2288 and imetelstat-treated cancer cells (Fig. 6 F–H). Finally, we tested whether UC2288 can inhibit tumor growth in vivo. Toward this end, we injected HCT116 and ACHN cells
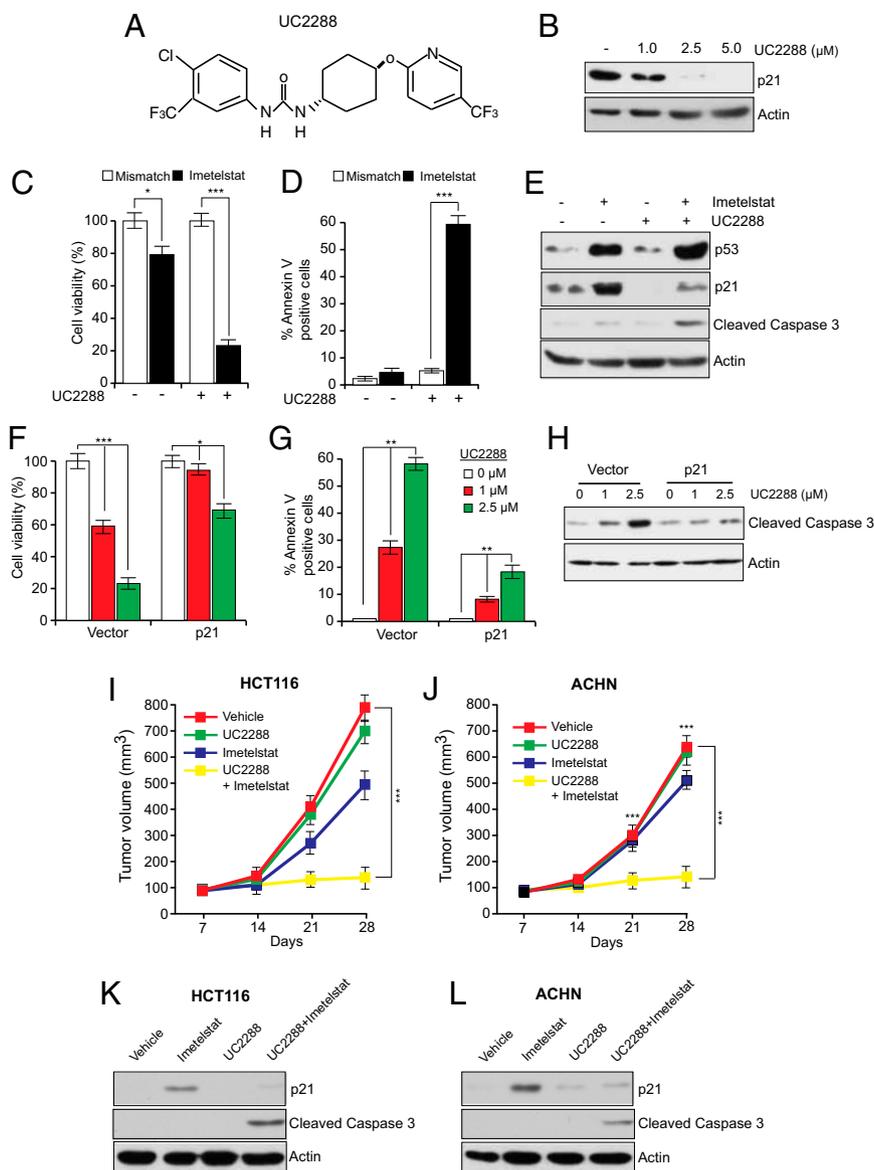

Fig. 6. Simultaneous pharmacological inhibition of p21 by UC2288 and telomerase prevents tumor growth in mice. (A) Chemical structure of UC2288. (B) Immunoblot of p21 expression in HCT116 cells treated with DMSO or with indicated concentrations of UC2288 for 24 h. (C) Relative cell viability measured by trypan blue exclusion assay of HCT116 cells treated with imetelstat, UC2288 (2.5 μM), or both. (D) % Annexin V–FITC–positive HCT116 cells treated with imetelstat and UC2288 was measured by FACS analysis. (E) Immunoblot for indicated proteins in HCT116 cells following treatment with U2288, imetelstat, or both. (F) Relative cell viability measured by trypan blue exclusion assay of imetelstat-treated HCT116 cells transfected with control or p21 expression vectors and then treated with UC2288. (G) % Annexin V–FITC–positive cells was measured by FACS analysis of imetelstat-treated HCT116 cells transfected with control or p21 expression vectors and then treated with UC2288. (H) Cleaved caspase 3 was measured by immunoblot in imetelstat-treated HCT116 cells transfected with control or p21 expression vectors and then treated with UC2288. (I) Average tumor volumes of HCT116 xenograft from mice treated with vehicle, UC2288 alone, imetelstat alone, or both drugs. **P < 0.001; ***P < 0.0001. (J) Average tumor volumes of ACHN xenograft from mice treated with vehicle, UC2288 alone, imetelstat alone, or both drugs. (K) Mouse-derived HCT116 xenograft tumors under indicated treatment conditions were analyzed for indicated proteins by immunoblot analysis. (L) Mouse-derived ACHN xenograft tumors under indicated treatment conditions were analyzed for indicated proteins by immunoblot analysis. *P < 0.01; **P < 0.001; ***P < 0.0001.

Gupta et al.

into the flanks of athymic nude mice and followed it by treatment with UC2288, imetelstat, or both drugs. Notably, combined treatment with UC2288 and imetelstat synergistically suppressed tumor growth (Fig. 6 I–L and *SI Appendix*, Table S2).

Toxicity analyses revealed that there were no significant differences in the body weight or ALT, AST, AP, whole blood counts, and renal activity markers in mice that were treated with imetelstat, UC2288, or both drugs, in comparison with the control group (*SI Appendix*, Fig. S15).

Targeting Tumors Containing Mutant p53 Following Pharmacological Restoration of p53 Activity. The results described above show that in the absence of p21, p53 and E2F1 cooperate to activate PUMA expression, which is necessary for apoptosis induction (Figs. 3 and 4). Accordingly, cells that lack functional p53 are less sensitive to imetelstat-mediated growth inhibition compared with cells containing wild-type p53 (Fig. 3J).

Approximately 50% of human cancers lack a functional p53 pathway, largely due to inactivating mutations in the p53 gene (41). We therefore asked whether simultaneous inhibition of telomerase and p21 could be adapted to treat cancers harboring p53 mutants. Previous studies have shown that the function of several different cancer-associated p53 mutants can be restored by treatment with small molecules such as CP-31398 (42, 43). CP-31398 alters the conformation of p53, thereby promoting its ability to bind to DNA (42, 43). As expected, treatment of p53 mutant cancer cell lines DLD1 (Ser241Phe), SW480 (Arg273His and Pro309Ser), and A375.S2 (Arg249Ser) with CP-31398 restored p53 activity, as evidenced by increased expression of its transcriptional target p21 (Fig. 7A). Next, using shRNAs, we knocked down *p21* in DLD1 and A375.S2 cells (Fig. 7B) and treated these cells with imetelstat and CP-31398. Treatment with both CP-31398 and imetelstat inhibited the growth of DLD1 and A375 cells expressing a *p21* shRNA more strongly compared with
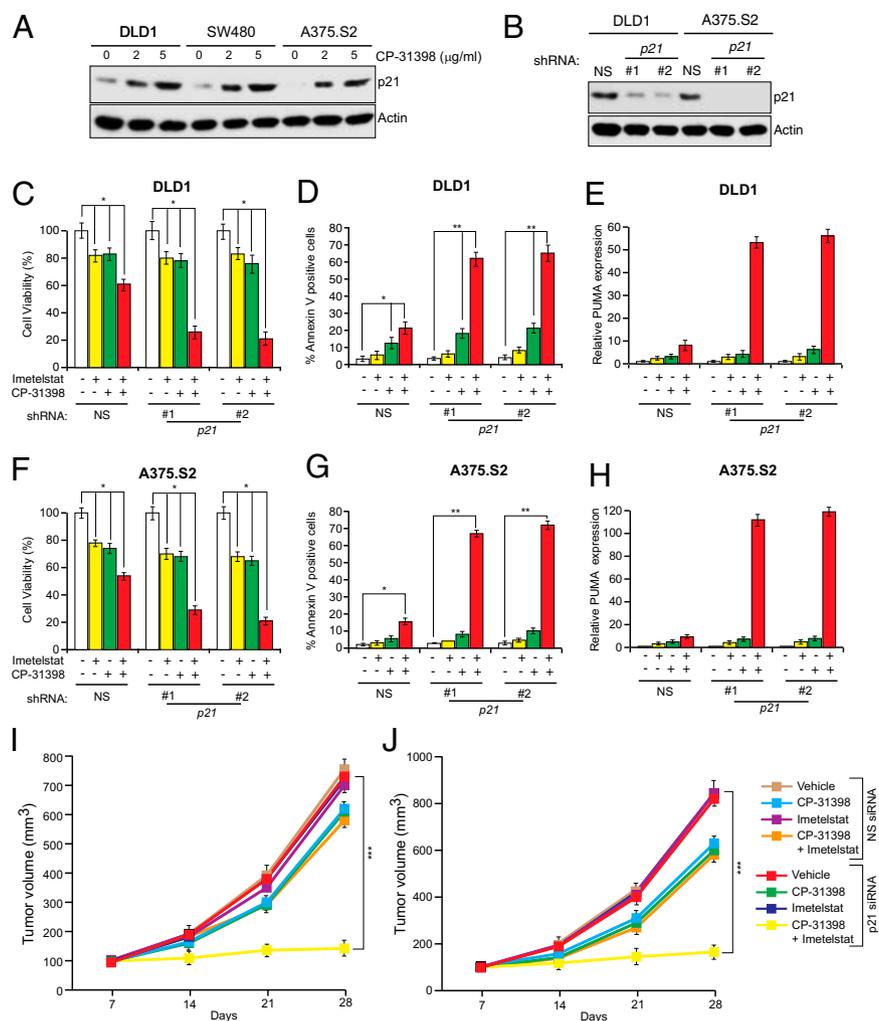

Fig. 7. Pharmacological restoration of p53 activity allows for the targeting of p53 mutant cancers by simultaneous p21 and telomerase inhibition. (A) Indicated p53 mutant cancer cell lines were treated at indicated concentrations of CP-31398 and analyzed for p21 expression by immunoblot. Actin was used as a loading control. (B) Indicated p53 mutant cancer cell lines expressing either an NS shRNA or shRNA targeting p21 were analyzed for p21 expression by immunoblot. Actin was used as a loading control. (C and F) DLD1 cells (C) or A375.S2 cells (F) expressing indicated shRNAs were treated with mismatch oligonucleotide or imetelstat for 6 wk and were either untreated or treated with CP-31398 for 2 d. Cell viability was measured by trypan blue assay, and relative cell viability is plotted. (D and G) DLD1 cells (D) or A375.S2 cells (G) expressing indicated shRNAs were treated with mismatch oligonucleotide or imetelstat for 6 wk and were either untreated or treated with CP-31398 for 2 d. Apoptosis was measured by Annexin V staining, and % apoptosis is plotted. (E and H) DLD1 cells (E) or A375.S2 cells (H) expressing indicated shRNAs were treated with mismatch oligonucleotide or imetelstat for 6 wk and were either untreated or treated with CP-31398 for 2 d. PUMA expression was measured by qRT-PCR. (I and J) Average tumor volumes of DLD1 xenograft (I) or A375.S2 (J) from mice treated with vehicle, CP-31398 alone, imetelstat alone, or both drugs with simultaneous treatment with nanoparticles with nonspecific or *p21* siRNA are shown. *$P < 0.01$; **$P < 0.001$; ***$P < 0.0001$.

cells expressing a nonspecific shRNA (Fig. 7 *C* and *F* and *SI Appendix*, Fig. S16). Growth inhibition correlated with increased apoptosis (Fig. 7 *D* and *G*) and significantly higher PUMA activation (Fig. 7 *E* and *H*). Finally, we tested this approach for suppressing tumor growth in vivo. We found that addition of CP-31398 combined with simultaneous inhibition of telomerase and p21 substantially suppressed growth of tumors containing mutant p53 (Fig. 7 *I* and *J*). Collectively, these results show that simultaneous inhibition of telomerase and p21 can also be used to treat cancers containing mutant p53.

Discussion

A large majority of diverse tumor types express telomerase, which is critical for cancer cell survival. Thus, inhibition of telomerase activity can block tumor cell growth both in vitro and in vivo. Due to such widespread expression and the requirement of telomerase for cancer cell survival, telomerase inhibitors can, in principle, be used to treat a broad spectrum of cancer types. In fact, telomerase inhibitors such as imetelstat have advanced into the clinic for the treatment of human cancers. However, for several reasons, single-agent telomerase therapies have not proven effective. First, because telomere shortening and consequential tumor growth inhibition require many cell divisions, single-agent telomerase inhibitors require substantial time to significantly decrease tumor growth. Second, telomerase inhibition typically results in only a cytostatic effect, which allows tumor cells to acquire secondary genetic and epigenetic alterations resulting in drug resistance. Finally, single-agent telomerase therapeutics often fail due to activation of ALT pathways, which bypasses the requirement for telomerase (25).

In this report, we have studied the role of p21 in telomerase inhibition-mediated growth suppression. We found that p21 loss increases apoptosis induction following telomerase inhibition in a variety of cancer cell lines and mouse xenografts. We further showed that apoptosis induction is specifically due to up-regulation of *PUMA* expression and that up-regulation of *PUMA* expression is dependent upon both p53 and E2F1. Although our results are consistent with other studies reporting that p21 can regulate apoptosis (9–13), the specific apoptotic mechanism we identify has not been previously described.

Previous studies have shown that p21 loss sensitizes cells to DNA-damage–induced apoptosis (9–13). In our experiments, treatment of cells with imetelstat induces a DNA damage response, which upon simultaneous loss of p21, results in apoptosis. Thus, the loss of p21 effectively converts the response of imetelstat from simple growth inhibition to apoptosis. According to this mechanism, the specificity of growth inhibition is due to imetelstat, which will selectively induce a DNA damage response

in telomerase-positive cancer cells but not telomerase-negative normal cells.

Our finding that p21 is required to prevent apoptosis following telomerase inhibition reveals a critical genetic vulnerability of telomerase-expressing cancer cells. Accordingly, using both RNAi-based and pharmacological approaches, we showed that simultaneous inhibition of p21 and telomerase induces apoptosis in telomerase-positive human cancer cell lines and synergistically suppresses tumor growth. Specifically, we found that two unrelated pharmacological inhibitors of p21, sorafenib and UC2288, could function synergistically with imetelstat. Notably, in both cases, growth inhibition could be counteracted by ectopic expression of p21, indicating that sorafenib and UC2288 functioned by inhibiting p21 and not through an off-target effect. The induction of apoptosis by simultaneous inhibition of p21 and telomerase may greatly reduce the likelihood that resistance to telomerase inhibitors will develop through additional secondary genetic alterations or activation of ALT pathways. Finally, we show that simultaneous inhibition of telomerase and p21 also suppresses growth of tumors containing mutant p53 following pharmacological restoration of p53 activity.

Overall, we anticipate that simultaneous inhibition of telomerase and p21 can potentially overcome the current limitation of single-agent telomerase therapeutics and provide an effective method to treat a large number of cancers that rely on telomerase activity for survival, including the p53 mutant cancers.

Materials and Methods

Materials and procedures for all experiments are supplied in *SI Appendix*. Included in *SI Appendix* are the mammalian cell culture procedures, details regarding tumorigenesis assay, protocols for TRAP assay to measure telomerase activity, Terminal Restriction Fragment analysis to measure telomere length, and ALT activity assay to monitor C-Circle amplification. Also provided are additional figures and tables providing p16 status of the cell lines used in our study, primer sequence information and antibody details used for immunolotting, and the statistical analyses of drug combinations to establish synergistic effects.

1. Blackburn EH, Collins K (2011) Telomerase: An RNP enzyme synthesizes DNA. *Cold Spring Harb Perspect Biol* 3(5).
2. Shay JW, Wright WE (2011) Role of telomeres and telomerase in cancer. *Semin Cancer Biol* 21(6):349–353.
3. Hahn WC, et al. (1999) Inhibition of telomerase limits the growth of human cancer cells. *Nat Med* 5(10):1164–1170.
4. Chin L, et al. (1999) p53 deficiency rescues the adverse effects of telomere loss and cooperates with telomere dysfunction to accelerate carcinogenesis. *Cell* 97(4):527–538.
5. el-Deiry WS, et al. (1993) WAF1, a potential mediator of p53 tumor suppression. *Cell* 75(4):817–825.
6. Harper JW, Adami GR, Wei N, Keyomarsi K, Elledge SJ (1993) The p21 Cdk-interacting protein Cip1 is a potent inhibitor of G1 cyclin-dependent kinases. *Cell* 75(4):805–816.
7. Polyak K, Waldman T, He TC, Kinzler KW, Vogelstein B (1996) Genetic determinants of p53-induced apoptosis and growth arrest. *Genes Dev* 10(15):1945–1952.
8. Waldman T, Kinzler KW, Vogelstein B (1995) p21 is necessary for the p53-mediated G1 arrest in human cancer cells. *Cancer Res* 55(22):5187–5190.
9. Javelaud D, Besancon F (2002) Inactivation of p21WAF1 sensitizes cells to apoptosis via an increase of both p14ARF and p53 levels and an alteration of the Bax/Bcl-2 ratio. *J Biol Chem* 277(40):37949–37954.
10. Broude EV, et al. (2007) p21 (CDKN1A) is a negative regulator of p53 stability. *Cell Cycle* 6(12):1468–1471.
11. Xia M, Knezevic D, Vassilev LT (2011) p21 does not protect cancer cells from apoptosis induced by nongenotoxic p53 activation. *Oncogene* 30(3):346–355.
12. Dong C, Li Q, Lyu SC, Krensky AM, Clayberger C (2005) A novel apoptosis pathway activated by the carboxyl terminus of p21. *Blood* 105(3):1187–1194.
13. Chen Y, Zhang L, Jones KA (2011) SKIP counteracts p53-mediated apoptosis via selective regulation of p21Cip1 mRNA splicing. *Genes Dev* 25(7):701–716.
14. Röth A, Harley CB, Baerlocher GM (2010) Imetelstat (GRN163L)—Telomerase-based cancer therapy. *Recent Results Cancer Res* 184:221–234.
15. Macleod KF, et al. (1995) p53-dependent and independent expression of p21 during cell growth, differentiation, and DNA damage. *Genes Dev* 9(8):935–944.
16. Bunz F, et al. (1998) Requirement for p53 and p21 to sustain G2 arrest after DNA damage. *Science* 282(5393):1497–1501.
17. Goldberg M, et al. (2003) MDC1 is required for the intra-S-phase DNA damage checkpoint. *Nature* 421(6926):952–956.
18. Lou Z, Minter-Dykhouse K, Wu X, Chen J (2003) MDC1 is coupled to activated CHK2 in mammalian DNA damage response pathways. *Nature* 421(6926):957–961.
19. Stewart GS, Wang B, Bignell CR, Taylor AM, Elledge SJ (2003) MDC1 is a mediator of the mammalian DNA damage checkpoint. *Nature* 421(6926):961–966.
20. Dimitrova N, de Lange T (2006) MDC1 accelerates nonhomologous end-joining of dysfunctional telomeres. *Genes Dev* 20(23):3238–3243.
21. Zhu XD, Küster B, Mann M, Petrini JH, de Lange T (2000) Cell-cycle-regulated association of RAD50/MRE11/NBS1 with TRF2 and human telomeres. *Nat Genet* 25(3):347–352.
22. Kubo A, et al. (1999) The p16 status of tumor cell lines identifies small molecule inhibitors specific for cyclin-dependent kinase 4. *Clin Cancer Res* 5(12):4279–4286.

23. Lee EJ, et al. (2008) Histone deacetylase inhibitor scriptaid induces cell cycle arrest and epigenetic change in colon cancer cells. *Int J Oncol* 33(4):767–776.

24. Cesare AJ, Reddel RR (2010) Alternative lengthening of telomeres: Models, mechanisms and implications. *Nat Rev Genet* 11(5):319–330.

25. Hu J, et al. (2012) Antitelomerase therapy provokes ALT and mitochondrial adaptive mechanisms in cancer. *Cell* 148(4):651–663.

26. Henson JD, et al. (2009) DNA C-circles are specific and quantifiable markers of alternative-lengthening-of-telomeres activity. *Nat Biotechnol* 27(12):1181–1185.

27. Scheel C, et al. (2001) Alternative lengthening of telomeres is associated with chromosomal instability in osteosarcomas. *Oncogene* 20(29):3835–3844.

28. Miyashita T, Reed JC (1995) Tumor suppressor p53 is a direct transcriptional activator of the human bax gene. *Cell* 80(2):293–299.

29. Polyak K, Xia Y, Zweier JL, Kinzler KW, Vogelstein B (1997) A model for p53-induced apoptosis. *Nature* 389(6648):300–305.

30. Nakano K, Vousden KH (2001) PUMA, a novel proapoptotic gene, is induced by p53. *Mol Cell* 7(3):683–694.

31. Degenhardt K, Chen G, Lindsten T, White E (2002) BAX and BAK mediate p53-independent suppression of tumorigenesis. *Cancer Cell* 2(3):193–203.

32. Villunger A, et al. (2003) p53- and drug-induced apoptotic responses mediated by BH3-only proteins puma and noxa. *Science* 302(5647):1036–1038.

33. Carnevale J, Palander O, Seifried LA, Dick FA (2012) DNA damage signals through differentially modified E2F1 molecules to induce apoptosis. *Mol Cell Biol* 32(5):900–912.

34. Hershko T, Ginsberg D (2004) Up-regulation of Bcl-2 homology 3 (BH3)-only proteins by E2F1 mediates apoptosis. *J Biol Chem* 279(10):8627–8634.

35. Wang Y, Shen MF, Chang S (2011) Essential roles for Pot1b in HSC self-renewal and survival. *Blood* 118(23):6068–6077.

36. Woodrow KA, et al. (2009) Intravaginal gene silencing using biodegradable polymer nanoparticles densely loaded with small-interfering RNA. *Nat Mater* 8(6):526–533.

37. Cheng CJ, Saltzman WM (2011) Enhanced siRNA delivery into cells by exploiting the synergy between targeting ligands and cell-penetrating peptides. *Biomaterials* 32(26):6194–6203.

38. Inoue H, Hwang SH, Wecksler AT, Hammock BD, Weiss RH (2011) Sorafenib attenuates p21 in kidney cancer cells and augments cell death in combination with DNA-damaging chemotherapy. *Cancer Biol Ther* 12(9):827–836.

39. Wilhelm SM, et al. (2008) Preclinical overview of sorafenib, a multikinase inhibitor that targets both Raf and VEGF and PDGF receptor tyrosine kinase signaling. *Mol Cancer Ther* 7(10):3129–3140.

40. Wettersten HI, et al. (2013) A novel p21 attenuator which is structurally related to sorafenib. *Cancer Biol Ther* 14(3):278–285.

41. Brown CJ, Lain S, Verma CS, Fersht AR, Lane DP (2009) Awakening guardian angels: Drugging the p53 pathway. *Nat Rev Cancer* 9(12):862–873.

42. Foster BA, Coffey HA, Morin MJ, Rastinejad F (1999) Pharmacological rescue of mutant p53 conformation and function. *Science* 286(5449):2507–2510.

43. Takimoto R, et al. (2002) The mutant p53-conformation modifying drug, CP-31398, can induce apoptosis of human cancer cells and can stabilize wild-type p53 protein. *Cancer Biol Ther* 1(1):47–55.